Downstream Effects of Photoreceptor Degeneration and Electrical Retinal Stimulation on Visual Cortex Macrostructure and Function

Beomseo Koo, Ph.D. University of Michigan Biomedical Engineering Ann Arbor, USA beomkoo@umich.edu James Weiland, Ph.D.
University of Michigan
Biomedical Engineering
Ann Arbor, USA
weiland@med.umich.edu

Abstract— Visual prostheses are a possible treatment for retinal degenerate conditions. Research in visual protheses and blindness should consider the effect of retinal electric stimulation on the central visual pathway in respect to cortical structure and function. Transcorneal Electric Stimulation was used electrically activate the immunohistochemistry analysis of visual cortex was performed. Cortical layer thickness of primary visual cortex after photoreceptor degeneration in P23H rats was maintained compared to sighted rats at ages P120, P180, and P360. Transcorneal stimulation applied weekly or twice weekly did not results in differences in cortical thickness. C-Fos (a biomarker of neural activity) showed a weak trend towards reduced expression in cortex corresponding to retinal stimulation, counter to our expectation.

Keywords—Retinal Prosthesis, Visual Prosthesis, Artificial Vision, Retinitis Pigmentosa, Immunohistochemistry, Transcorneal Electric Stimulation

I. INTRODUCTION

Blindness and visual impairment are major public health concerns [1]. Given the reliance on vision to travel and interact with the physical world, vision loss is associated with lowered independence and quality-of-life [1]. Retinitis Pigmentosa (RP, a collective term for a heterogenous inherited retinopathy) has a prevalence of 1-in-4000 worldwide, and often results in severe vision loss [2, 3].

Artificial vision is currently of interest in those that have lost sight from RP, and is steadily growing to other vision impairment sources such as Age-Related Macular Degeneration, Diabetic Retinopathy, and Glaucoma. One retinal prosthesis has FDA approval for clinical use and cortical visual prostheses are under evaluation in clinical studies [4, 5, 6]. Relatively little work has involved cortical structure after retinal degeneration, and even less after using electric stimulation for sensory stimulation.

The brain is a highly adaptive system, and sensory information is amongst the most impactful stimuli that shape the brain. Blindness acquired in adulthood, typical of RP, causes functional and structural changes in the brain in spite of relatively reduced plasticity in adulthood. Clinical MRI studies of adult blindness have revealed downstream cascade effects of vision loss. Cross-modal plasticity is prevalent in individuals with vision loss, with seemingly even distribution of sound or touch responses evoked in V1 [7]. In a small trial of three Argus II implant patients, V1 light evoked responses increased after 6 months of retinal implant use, suggesting that electrical stimulation may improve cortical function [8, 9]. Artificial sensory stimulation may access similar cortical

reorganization measures that negative and positive vision outcomes utilize.

Here, we attempt to define structural and functional changes in the brain from progressive vision loss in a rat model of RP. Primary visual cortex monocular region (V1m) was investigated because of its role in cross-modal plasticity and its use in cortical visual prosthesis. Retinal ganglion cell activation using Transcorneal Electric Stimulation (TES) was performed to drive further changes in neural function and structure due to retinal activation. We utilized a rat animal model that exhibits one genetic defect under the RP umbrella, P23H [10]. These rats were studied at different age timepoints to compare the brain's state during progressive degeneration. We observed two labels: c-Fos and NeuN to determine the functional and structural changes in the rat brain with or without repeated retinal electric stimulation.

II. METHODS

A. Animal Care and Use

Pigmented P23H-1 rats were bred through the University of Michigan Unit for Laboratory Animal Medicine's Animal Husbandry by crossing an autosomal-dominant Sprague Dawley rat with the P23H mutation (SD-Tg(P23H)1Lav homozygote (RRRC, USA)) with a Long-Evans rat (Charles River, USA). Since the P23H mutation is dominant, LE-P23H-1 offspring all experience progressive and severe retinal degeneration [10]. LE-P23H-1 Rats of the P120, P180, and P360 age groups (n = 10, 10, and 9 at P120, P180, and P360, respectively) were used. The retinal degeneration progression of the P23H cohort has been defined previously using OCT and cortical recording [11]. Long-Evans rats, aged until P400 (N = 4), were used as a fully-sighted comparison group. All animal husbandry, surgical, and experimental procedures were approved by the Institutional Animal Care and Use Committee (IACUC) of University of Michigan.

B. Surgery and Artificial Vision Stimulation

To assess the presence of electric stimulation activating the retinal ganglion cells, most animals that were under the artificial vision treatment group were implanted with cortical recording screws (n = 6, 6, 4, respectively for P120, P180, and P360). Animals were implanted with cortical recording screws as previously mentioned [11].

To simulate artificial stimulation treatment, weekly TES was performed on LE-P23H-1 animals ($N=8,\ 8,\ 6$, respectively for P120, P180, and P360). All implanted P120 and P180 animals received weekly TES, and implanted P360 animals received stimulation twice weekly. The animal was anesthetized with an intraperitoneal injection of

Research supported by National Science Foundation CBET 1343193, CBET 2129817

ketamine/xylazine cocktail (80 mg/kg and 8 mg/kg, respectively). Two drops of proparacaine were applied to the right eye (Akorn, US). After proparacaine takes effect, balanced salt solution (BSS) drops were applied to clean the eye, and a platinum/iridium (Pt/Ir) wire loop was held above the cornea. A drop of BSS was used to create electrical contact between the cornea and the Pt/Ir wire loop. A stainless-steel wire was placed between the gum and inner lip of the animal as the current return electrode. The Pt/Ir wire loop and the stainless-steel wire were connected to the Plexon PlexStim System (Plexon, USA). 20 minutes of 800 μ A, 2 Hz, 1 ms per phase, cathodic-first, bi-phasic pulses were applied to the target eye. Voltage transient output during the 20-minute stimulation session and post-processed electrophysiology verified the stimulation [11].

C. Histology

Animals at endpoint were put under ketamine/xylazine anesthesia. 20 minutes of TES was applied as previously described. Afterwards, the animal was placed back in the home cage to rest for 1 hour to allow for c-Fos expression [12]. The animal was put under 5% isoflurane until breathing cessation and complete absence of hind-limb pinch response. The intraperitoneal cavity was opened, the lung punctured to ensure euthanasia, and initial intracardial perfusion of cold 1X PBS was applied. When the perfusate was clear, intracardial perfusion of 4% paraformaldehyde (PFA) was performed to fix the cortical tissue. The extracted brain remained overnight in 4% PFA for further fixation and moved to 1X PBS with 0.01% Sodium Azide for preservation.

Prior to sectioning, the brain was transferred to a 15% sucrose in 1X PBS solution for 24 hours and 30% sucrose in 1x PBS solution for 24 hours. The brain was removed from solution and dried with a Kimwipe (Kimberly-Clark, USA). The brain's frontal lobe and cerebellum were trimmed with a razor blade and a fiducial hole was made through the ventralright quadrant, avoiding the cortex layers, using a 100 µL pipette tip. The brain was submerged in OCT solution (Fisher Scientific, USA) for 10 minutes. The brain was transferred to a cryomold, filled with OCT, and placed in the -20° C cryostat chamber for 15 minutes. The frozen OCT block was placed on a cryosection stage with OCT applied. Coronal, 100 µm thick sections of the brain were made using a Cryostar NX50/70 (Fisher Scientific, USA). The slices were transferred to a 14-well plate with 1X PBS with 0.01% Sodium Azide.

Slices near -6 mm from bregma were chosen using the "Rat Brain Atlas" [13]. Slices at this position show clear separation of the corpus callosum while containing V1. Slices were transferred to a 9-well Pyrex glass spot plate (Fisher Scientific, 13-748B, USA). The slices were submerged twice in 6 mg/mL Sodium Borohydride (Sigma-Aldrich, USA) solution for 15 minutes to quench autofluorescence [14]. The slices were rinsed with 1X PBS three times, 5 minutes each. The slices were blocked with 4% Normal Goat Serum (Southern Biotech, USA), 0.6% Triton-X (Sigma-Adrich, USA) in 1X PBS solution for 1 hour. The slices were rinsed three time with 1X PBS, 1 minute each. Primary antibodies, 1:500 Rabbit anti-c-Fos, 1:500 Guinea-Pig anti-VGluT2, and 1:500 Mouse monoclonal anti-NeuN (Synaptic Systems, 226 003, 135 404, 266 011, Germany), in 4% Normal Goat Serum, 0.2% Triton-X in 1X PBS solution was applied overnight.

On the second day, the slices were rinsed with 1X PBS four times, 15 minutes each. Secondary antibodies, 1:1000 Goat anti-Rabbit Alexa Fluor Plus 647 (Invitrogen, A32733, USA), 1:1000 Goat anti-Guinea-Pig Alexa Fluor 488 (Jackson Immunoresearch Laboratories Inc., 106-545-003, USA), 1:1000 Goat Anti-Mouse Alexa Fluor 594 (Jackson Immunoresearch Laboratories Inc., 115-585-003, USA), and 1:500 DAPI (Thermo Fisher Scientific, D1306, USA) in 4% Normal Goat Serum, 0.2% Triton-X in 1X PBS solution was applied for 1 hour. The secondary antibodies were made in a dark room and protected with aluminum foil. The slices were rinsed with 1X PBS three times, 15 minutes each while covered with aluminum foil.

Stained slices were transported to frosted microscope slide (Fisher Scientific, 12-544-2, USA). Fluoromount-G (Southern Biotech, USA) was applied over the slices. #1.5 Coverslip (Bioscience Tools, USA) was applied over the slices and media, and the edges were seal with nail polish (Electron Microscopy Sciences, 72180, USA).

The stained slices were imaged with a Nikon A1R Confocal Microscope (Nikon, Japan). 305, 488, 546, 647 nm lasers were used. All labels were imaged with 20x magnification (1.25 $\mu m/pixel$ resolution), with a 2 \times 5 montage with 1.7 μm depth step-size. The montage included the cortex surface, the six V1m layers, and the white matter below. A constant laser parameter for each laser wavelength was kept for all animals and their V1m hemispheres imaged.

D. Image Pre-processing

20x montage image-stacks were separated by label, converted to 8-bit, and exported to FiJi. Max-projection of the image-stack was made for each label. The NeuN and VGluT2 labels were overlayed for cortical layer segmentation. The c-Fos label image was aligned with the NeuN/VGluT2 image and both were cropped to a 1 mm width (800 pixels). Any noise, auto-fluorescent debris or folded meninges over cortical layers, outside and inside the tissue was manually removed.

E. Image Analysis

Cortical Layer Thickness

The NeuN/VGluT2 images were considered as 2-D matrices for analysis calculations. The cortical surface was the first row with a non-zero value for all image columns, and the resulting 1 × 800 vector was smoothed. A user semiautomatically defined five layers: Layer I, II/III, IV, V, and VI **MATLAB** using Image Segmenter (imageSegmenter). Using the graph cut method, the user defined a foreground and background in the NeuN/VGluT2 image of the desired cortical layer. The app generates an approximate mask, using NeuN and VGluT2 fluorescence intensity and density as semantic information. Two users created each layer mask separately. The cortical layer thickness data was average between the two users and compared between animal age groups, between TES and naïve groups, and between LE-P23H-1 and LE groups.

c-Fos Punctate Analysis

The cortical layer masks from NeuN/VGluT2 images and the 20x c-Fos label image were imported to MATLAB. Two threshold images were created: >60/256 and >35/256 image intensity. The >60/256 image included the bright c-Fos punctate core and the >35/256 contains the outer region. The >60/256 image was inputted into a size threshold of 5-pixel

area (bwareaopen, 7.5 μm^2) and the >35/256 image a 30-pixel area threshold (45 μm^2). A c-Fos punctate contained both components, so a comparison mask was made. The resulting mask was inputted to (regionprops) to create a list of centroid maps. Watershed processing was performed for each centroid's image content to separate overlapping c-Fos punctate regions (with adequate size thresholding afterwards). Punctate count of each layer per animal were compared across animal age groups, between TES and naïve groups, and between genetic groups.

Statistical Analysis

Cortical layer thickness and c-Fos punctate counts were analyzed using linear mixed model with equation (Thickness/Punctate Count) \sim Animal Age * TES/Naïve * Left/Right +(1|ID). Animal age was a categorical value with P120, P180, P360, and Long-Evans groups, TES/Naïve was a categorical value, and Left/Right was a categorical value with left (contralateral to TES) or right (ipsilateral) brain hemisphere. Animal ID was used as a random effect in the regression equation. All linear mixed models started with LE-P23H-1, P120, and LEFT as the starting reference point. Significance was measured at $\alpha=0.05$.

III. RESULTS

All animals exhibited the six cortical layers' stratification regardless of age or genetic condition. Overall, total cortical thickness did not differ significantly between animal groups using linear mixed model (Fig. 1). Linear mixed model in individual cortical layers revealed only P120:Left-Hemisphere:TES→P180:Right-Hemisphere:Naïve interaction in Layer IV was significant (p = 0.016, [14.523 135.05] 95% Confidence Interval, Fig. 2). Given the lack of other trends, we considered this result to be spurious.

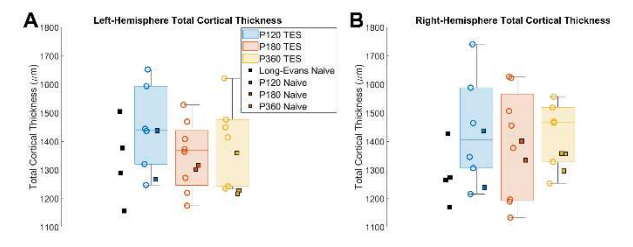


Figure 1: Total cortical layer thickness of left (contralateral to TES) and right hemisphere of V1m. Filled squares: Naïve animals, Empty circles:

Animals that received TES.

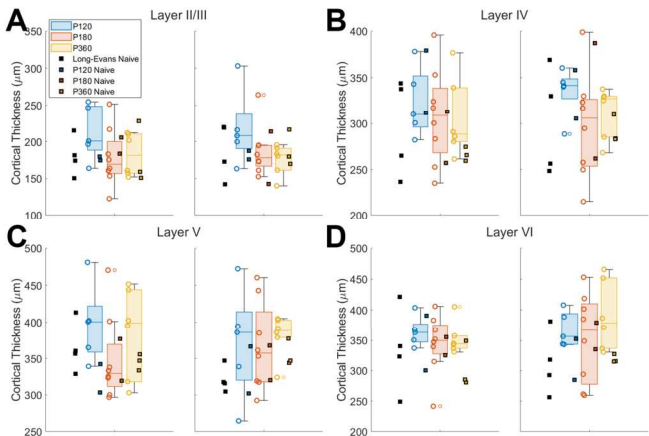


Figure 2: Cortical layer thickness per layer and hemisphere. Layer I was omitted for brevity. (A) Layer II/III, (B) Layer IV, (C) Layer V, (D) Layer

For the c-fos punctate analysis, four animals were excluded: one was excluded for poor staining quality leading to no detectable c-fos fluorescence, one had excessive adhesion of primary Rabbit anti-c-Fos antibodies leading to poor contrast, and two were excluded due to data corruption of images. C-fos punctate count measured using 20x c-Fos images of LE-P23H-1 V1m returned some significant interaction in layers of V1m (Fig. 3, Table 1). An interaction between the left and right hemisphere was seen in Layer II/III, Layer IV, and Layer VI where the left hemisphere had less punctate count detected compared to right hemisphere. Age-related interactions were seen in Layer I, Layer IV, Layer V, and Layer VI. The main trend was that P120 had more punctate count compared to P180 and P360 in the previously mentioned laminar layers.

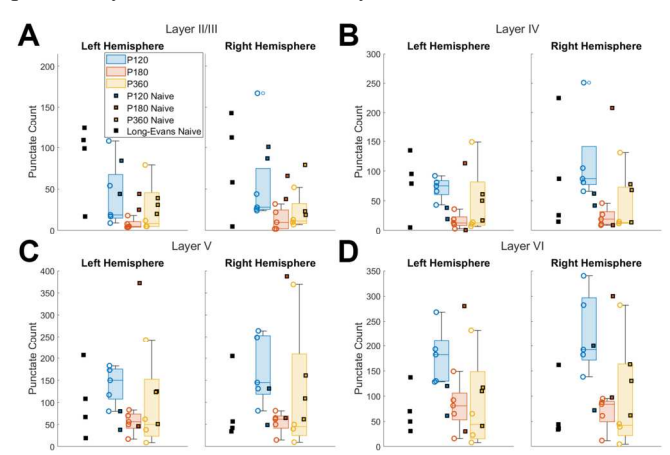


Figure 3: C-Fos punctate count per layer and hemisphere Layer I was omitted for brevity. (A) Layer II/III, (B) Layer IV, (C) Layer V, (D) Layer

TABLE I. LIST OF SIGNIFICANT C-FOS INTERACTIONS

Interaction	p-value	95% Confidence Interval		Did Naïve Group by itself have the same interaction?
Layer II/III				
Left→Right Hemisphere	2.97e ⁻²	[1.733	31.07]	Yes
Layer IV				
Left→Right Hemisphere	2.36e ⁻³	[17.95	75.25]	No
Layer VI				
Left→Right Hemisphere	1.53e ⁻²	[9.594	83.61]	Yes

IV. DISCUSSION

Cortical Layer Thickness

Cortical Thickness measure did not change significantly between animal age groups. The results are not consistent with the assertion made in a clinical MRI study performed for RP [15], and total cortical thickness of P30 and P230 P23H-1 homozygote albino rats [16]. Reported loss of visual field correlated with reduced gray matter volume, and the gray matter reduction was attributed to reduction in V1's peripheral vision regions. The differing results may be affected by the disparity between rat retina and human retina (i.e., rat retina lacking a macula/fovea). Due to cortical magnification, more cortical area contributes to processing central vision compared to peripheral vision in humans. Degeneration into macular regions may result in a greater effect in gray matter reduction from the disuse-driven neural atrophy discussed by [15]. Rats do not have as disproportional cortical magnification as humans do [17], and disuse atrophy may be mitigated from

cross-modal plasticity. For the albino P23H-1, the homozygote expression of P23H result in greater loss of retinal thickness; albino P23H-1 P30 is equivalent to LE-P23H-1 P60 [18]. Long-Evans rats are considered young adults around P60, so at P30 albino P23H rats may have experienced a greater disuse atrophy from the more impressionable cortical network.

B. c-Fos Punctate

C-fos imaging revealed a significant interaction between Left→Right Hemisphere for Layer II/III, Layer IV, and Layer VI in linear mixed models. The trend showed that the left hemisphere (contralateral to TES application) had lower levels of detected c-fos punctate count compared to the right hemisphere. The effect was unexpected and the mechanism is uncertain.

The effect may indicate that corneal stimulation led to mitigation of increased spontaneous activity present in retinal degenerate animals [19], even after cessation of stimulation. Therefore, the overall activity of the cortex is less, leading to reduced c-Fos expression, but only in the cortex receiving electrically induced retinal input. The stimulus rate used (2 Hz) is consistent with rates found to create long-term depression (1 – 4 Hz) [20]. An alternative explanation, albeit less interesting, is that variation in IHC processing resulted in differences in expression that was not due to any difference in neural activity.

Naïve animals having the same interaction for Layer II/III and Layer VI, but not for Layer IV, adds further complexity to the reduction of spontaneous activity. The result may implicate a possible cross-modal and subcortical-cortical connection dynamics induced by TES. Layer II/III is directly connected to other sensory cortices: primary auditory [21] and primary somatosensory [22, 23] cortices. Corneal stimulation may create activity in somatosensory cortex, which could influence Layer II/III and Layer VI of primary visual cortex indirectly rather than propagating through Layer IV. Layer IV however, has no cross-modal circuitry, and the lack of naïve animal interaction may indicate a possible direct, long-term effect of weekly TES application.

In summary, TES applied weekly or twice-weekly to the cornea in retinal degenerate rats did not alter cortical structure but may have altered cortical function.

REFERENCES

- [1] A. W. Scott, N. M. Bressler, S. Ffolkes, J. S. Wittenborn, and J. Jorkasky, "Public Attitudes About Eye and Vision Health," JAMA Ophthalmology, vol. 134, no. 10, pp. 1111–1118, Oct. 2016, doi: 10.1001/jamaophthalmol.2016.2627.
- [2] D. T. Hartong, E. L. Berson, and T. P. Dryja, "Retinitis pigmentosa," The Lancet, vol. 368, no. 9549, pp. 1795–1809, Nov. 2006.
- [3] J. D. Weiland and M. S. Humayun, "Retinal Prosthesis," IEEE Transactions on Biomedical Engineering, vol. 61, no. 5, pp. 1412– 1424, May 2014, doi: 10.1109/TBME.2014.2314733
- [4] K. Stingl et al., "Artificial vision with wirelessly powered subretinal electronic implant alpha-IMS," Proceedings of the Royal Society B: Biological Sciences, vol. 280, no. 1757, p. 20130077, Apr. 2013, doi: 10.1098/rspb.2013.0077
- [5] J. D. Weiland, S. T. Walston, and M. S. Humayun, "Electrical Stimulation of the Retina to Produce Artificial Vision," Annual Review of Vision Science, vol. 2, no. 1, pp. 273–294, 2016

- [6] D. Palanker, Y. Le Mer, S. Mohand-Said, and J. A. Sahel, "Simultaneous perception of prosthetic and natural vision in AMD patients," Nat Commun, vol. 13, no. 1, Art. No. 1, Jan. 2022, doi: 10.1038/s41467-022-28125-x
- [7] S. I. Cunningham, J. D. Weiland, P. Bao, and B. S. Tjan, "Visual cortex activation induced by tactile stimulation in late-blind individuals with retinitis pigmentosa," in 2011 Annual International Conference of the IEEE Engineering in Medicine and Biology Society, 2011, pp. 2841– 2844
- [8] E. Castaldi, G. M. Cicchini, L. Cinelli, L. Biagi, S. Rizzo, and M. C. Morrone, "Visual BOLD Response in Late Blind Subjects with Argus II Retinal Prosthesis," PLoS Biol., vol. 14, no. 10, p. e1002569, Oct. 2016
- [9] S. I. Cunningham et al., "Feasibility of Structural and Functional MRI Acquisition with Unpowered Implants in Argus II Retinal Prosthesis Patients: A Case Study," Trans. Vis. Sci. Tech., vol. 4, no. 6, pp. 6–6, Nov. 2015
- [10] E. Orhan et al., "Genotypic and Phenotypic Characterization of P23H Line 1 Rat Model," PLOS ONE, vol. 10, no. 5, p. e0127319, May 2015, doi: 10.1371/journal.pone.0127319
- [11] B. Koo and J. D. Weiland, "Progressive Retinal Degeneration Increases Cortical Response Latency of Light Stimulation but Not of Electric Stimulation," Translational Vision Science & Technology, vol. 11, no. 4, p. 19, Apr. 2022, doi: 10.1167/tvst.11.4.19
- [12] Gucht, Estel Van der, et al. "A New Cat Fos Antibody to Localize the Immediate Early Gene C-Fos in Mammalian Visual Cortex after Sensory Stimulation." Journal of Histochemistry & Cytochemistry, vol. 48, no. 5, May 2000, pp. 671–84. SAGE Journals,
- [13] Paxinos, George; Watson, Charles. The Rat Brain in Stereotaxic Coordinates London: Academic Press, 2007.
- [14] Clancy, B., and L. J. Cauller. "Reduction of Background Autofluorescence in Brain Sections Following Immersion in Sodium Borohydride." Journal of Neuroscience Methods, vol. 83, no. 2, Sept. 1998, pp. 97–102. ScienceDirect,
- [15] Rita Machado, Ana, et al. "Structure-Function Correlations in Retinitis Pigmentosa Patients with Partially Preserved Vision: A Voxel-Based Morphometry Study." Scientific Reports, vol. 7, no. 1, 1, Sept. 2017, p. 11411.
- [16] Martinez-Galan, Juan R., et al. "Pre- and Postsynaptic Alterations in the Visual Cortex of the P23H-1 Retinal Degeneration Rat Model." Frontiers in Neuroanatomy, vol. 16, Oct. 2022, p. 1000085. PubMed Central, https://doi.org/10.3389/fnana.2022.1000085. Gias, C., et al. "Retinotopy within Rat Primary Visual Cortex Using Optical Imaging." NeuroImage, vol. 24, no. 1, Jan. 2005, pp. 200–06. ScienceDirect
- [17] Lowe, Robert J., et al. "Influence of Eye Pigmentation on Retinal Degeneration in P23H and S334ter Mutant Rhodopsin Transgenic Rats." Experimental Eye Research, vol. 187, Oct. 2019, p. 107755. ScienceDirect, https://doi.org/10.1016/j.exer.2019.107755.
- [18] Wang, Yi, et al. "Spontaneous Neural Activity in the Primary Visual Cortex of Retinal Degenerated Rats." Neuroscience Letters, vol. 623, June 2016, pp. 42–46. ScienceDirect
- [19] Kirkwood, Alfred, and Mark F. Bear. "Homosynaptic long-term depression in the visual cortex." Journal of Neuroscience 14.5 (1994): 3404-3412.
- [20] Garner, Aleena R., and Georg B. Keller. "A Cortical Circuit for Audio-Visual Predictions." *Nature Neuroscience*, vol. 25, no. 1, 1, Jan. 2022, pp. 98–105.
- [21] Sieben, Kay, et al. "Neonatal Restriction of Tactile Inputs Leads to Long-Lasting Impairments of Cross-Modal Processing." PLOS Biology, vol. 13, no. 11, Nov. 2015, p. e1002304.
- [22] Henschke, Julia U., et al. "Possible Anatomical Pathways for Short-Latency Multisensory Integration Processes in Primary Sensory Cortices." Brain Structure and Function, vol. 220, no. 2, Mar. 2015, pp. 955–77.